



# Engineering characterisation of a shaken, single-use photobioreactor for early stage microalgae cultivation using *Chlorella sorokiniana*



E.O. Ojo, H. Auta, F. Baganz, G.J. Lye\*

The Advanced Centre for Biochemical Engineering, Department of Biochemical Engineering, University College London, Torrington Place, London WC1E 7JE, UK

## HIGHLIGHTS

- A shaken, single-use photobioreactor (SUPBr) was developed and characterised.
- Visualisation of fluid hydrodynamics showed in-phase and out-of-phase flow regimes.
- Growth kinetics of *C. sorokiniana* were comparable to those reported in other PBr types.
- Liquid fill volume and light path length had the highest impact on culture performance.
- The SUPBr aids rapid, early stage development of microalgae cultivation processes.

## ARTICLE INFO

### Article history:

Received 20 July 2014

Received in revised form 9 September 2014

Accepted 13 September 2014

Available online 28 September 2014

### Keywords:

Single-use photobioreactor

Orbital shaking

Fluid hydrodynamics

*Chlorella sorokiniana*

Fatty acid methyl esters

## ABSTRACT

This work describes the characterisation and culture performance of a novel, orbitally shaken, single-use photobioreactor (SUPBr) system for microalgae cultivation. The SUPBr mounted on an orbitally shaken platform was illuminated from below. Investigation of fluid hydrodynamics indicated a range of different flow regimes and the existence of 'in-phase' and 'out-of-phase' conditions. Quantification of the fluid mixing time ( $t_m$ ) indicated a decrease in  $t_m$  values with increasing shaking frequency up to 90 rpm and then approximately constant  $t_m$  values in the range 15–40 s. For batch cultivation of *Chlorella sorokiniana*, the highest biomass concentration achieved was  $6.6 \text{ g L}^{-1}$  at light intensity of  $180 \mu\text{mol m}^{-2} \text{ s}^{-1}$ . Doubling the total working volume resulted in 35–40% reduction in biomass yield while shaking frequency had little influence on culture kinetics and fatty methyl esters composition. Overall this work demonstrates the utility of the SUPBr for early stage development of algal cultivation processes.

© 2014 The Authors. Published by Elsevier Ltd. This is an open access article under the CC BY license (<http://creativecommons.org/licenses/by/3.0/>).

## 1. Introduction

Single-use bioreactors (SUBs) have found increasing applications in recent years (Hillig et al., 2014; Zhang et al., 2009). SUBs are typically made from polyethylene or polyester multi-layer films and are provided pre-sterilised by gamma irradiation (Singh, 1999) with working volumes in the range 1–2000 L (Brecht, 2009). The original SUBs operated on a slowly rocked platform designed to induce a wave-type motion in the culture fluid promoting mixing and gas mass transfer. The main applications include early stage mammalian cell culture process development and inoculum generation (Kalmbach et al., 2011; Oncül et al., 2009) at scales up to 500 L. The most recent SUB designs resemble conventional stirred tank bioreactors and are now commonly used for therapeutic antibody and vaccine production up to 2000 L scale.

For phototrophic microalgae cultivation under contained conditions, most modern photobioreactors (PBr) are based on air-lift designs with light being supplied externally or radiated internally (Chen et al., 2011; Ugwu et al., 2005). In addition to the requirements for good mixing and gas mass transfer, adequate light must be supplied to enable efficient photosynthesis. Since the penetration of light into a culture fluid follows an exponential decay function it is desirable to have short light paths at constant distance from the light source. In this regard orbital shaking of a single-use photobioreactor (SUPBr) bag could provide a number of advantages as illustrated in Fig. 1 since a shorter and more constant light path length is maintained.

This work describes the use of an orbitally shaken, single-use bag for phototrophic microalgae cultivation. In particular, the engineering characteristics of this novel SUB were addressed in order to establish how the hydrodynamic environment impacts on fluid mixing and algal growth. These studies build on a number of recent works, by ourselves and others, that have addressed fluid mixing in

\* Corresponding author.

E-mail address: [g.lye@ucl.ac.uk](mailto:g.lye@ucl.ac.uk) (G.J. Lye).

## Nomenclature

$A_{\text{pbr}}$	bioreactor illuminated surface area ( $\text{m}^2$ )	PUFA	poly-unsaturated fatty acids
$C_{\text{chl-a,b}}$	chlorophyll (a and b) ( $\text{mg L}^{-1}$ )	$r_G$	maximum daily biomass growth ( $\text{g L}^{-1} \text{d}^{-1}$ )
$C_{\text{ppc}}$	carotenoids concentration ( $\text{mg L}^{-1}$ )	SFA	saturated fatty acids
$d_o$	orbital shaking diameter (mm)	S/V	surface area to volume ratio
$H$	maximum height of the liquid (m)	SUPBr	single-use photobioreactor
$H_G$	enthalpy of dry biomass ( $\text{kJ g}_{\text{DCW}}^{-1}$ )	$t_1$	initial culture time (s)
$H_N$	normalised height	$t_2$	final culture time (s)
$H_o$	initial height of liquid (m)	$t_m$	mixing time (s)
IPAR	illuminated photosynthetic active radiation (400 <sub>nm</sub> –700 <sub>nm</sub> )	TBP	tris-base phosphate
$k_L a$	oxygen mass transfer coefficient ( $\text{h}^{-1}$ )	UFA	unsaturated fatty acids
LEDs	light emitting diodes	$V_1$	sample volume ( $\text{m}^3$ )
MUFA	monounsaturated fatty acids	$V_2$	extraction solvent volume ( $\text{m}^3$ )
$N$	shaking frequency (rpm)	$V_f$	fractional fill volume of total working volume
OD	optical density	$X_1$	initial dry cell weight ( $\text{g L}^{-1}$ )
PE	photosynthetic efficiency (%)	$X_2$	final dry cell weight ( $\text{g L}^{-1}$ )
		$Y_{\text{x,E}}$	biomass yield on photon energy ( $\text{g mol}^{-1}$ )

a range of orbitally shaken or rocked SUBs of different geometries and scales (Betts et al., 2006; Kalmbach et al., 2011; Micheletti et al., 2006; Oncül et al., 2009; Tan et al., 2011; Tissot et al., 2010). The shaken SUPBr is considered a useful tool for early stage microalgae cultivation increasing experimental throughput and reducing operating costs by overcoming the need for bioreactor cleaning and sterilisation (Lehmann et al., 2013; Singh, 1999). Rocked bags of the design used here are commercially available up to 500 L scale which is around the maximum scale envisaged for the SUPBr technology. Current industry practice with single-use technology is for scale-out manufacture (i.e. use of multiple intermediate scale photobioreactors) rather than direct scale-up. This would suggest the technology described here is best suited

to early stage microalgae strain evaluation or for high value product manufacture using microalgae.

## 2. Methods

### 2.1. Shaken single-use photobioreactor setup

The SUPBr consisted of a standard 2 L Biostat Cultibag™ (Sartorius Stedim Biotech., Göttingen, Germany), 27.5 by 55.5 cm, clamped by its ends on an orbitally shaken incubator platform (Infors HT, Basel, Switzerland). The platform was fitted with 260 warm white light emitting diodes (LEDs) immediately below the shaking platform and the bag had an illuminated surface area of 0.15  $\text{m}^2$  uninflated ( $A_{\text{pbr}}$ ). The SUPBr with working volume of 0.5–1 L, was shaken with orbital diameters from 12.5 to 50 mm and at shaking frequencies from 40 to 220 rpm. The SUPBr was inflated with a constant gas flow rate of 2  $\text{mL min}^{-1}$  controlled using air flow meters (Fisher Scientific, Loughborough, UK) and pressure valve regulators (Norgren, Manchester, UK). In order to enable online pH measurements during hydrodynamic experiments, a pH probe (PY-P22 Micro pH Electrode length 110 mm) was inserted in the centre port of the bag normally used for gas exchange.

### 2.2. Visualisation of fluid hydrodynamics

Investigation of fluid hydrodynamics in the orbitally shaken SUPBr was achieved using a DVR Fastcam (Photron, California, USA). This was mounted directly above the Cultibag™ at an inclination of 30–60° and the resolution was set at 640 × 480 pixels for all experiments. Two halogen red lamps (National Instruments, UK) were used to provide additional light for improved brightness and clearer focus. The camera was set to capture images at 125 fps over a period of 5 min, for each of the experimental runs. The images captured were stored for analysis using ImageJ software (<http://rsbweb.nih.gov/ij/>). Fluid mixing was visualised by adding food dyes (2% v/v) with an approximate injection time of 3 s. In-phase and out-of-phase flow regimes (Büchs et al., 2001) were determined by quantification of the height reached by the fluid during shaking using a digital camera (Finepix, JX200, China). The maximum liquid height attained at various shaking conditions were normalised according to Eq. (1):

$$H_N = \frac{H - H_o}{H_o} \quad (1)$$

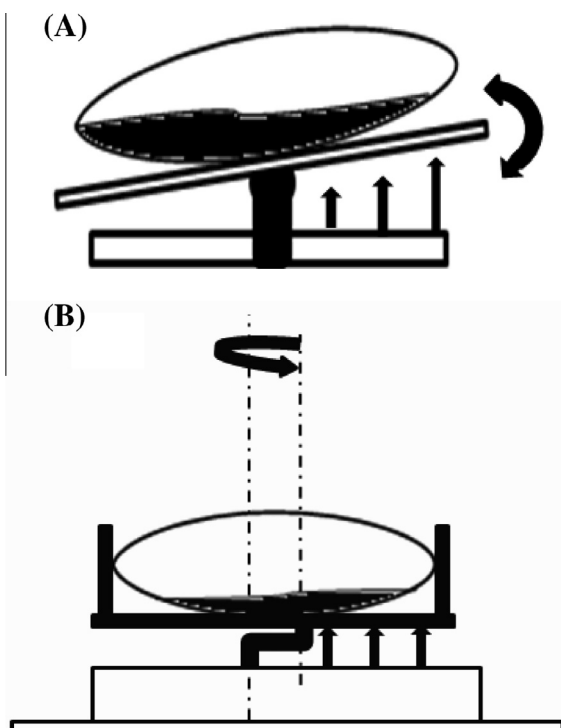


**Fig. 1.** Comparison of (A) a rocked, wave-generating platform and (B) an orbitally shaken platform for single-use photobioreactor agitation. Arrows indicate the more uniform and consistent light path-length achieved using orbital shaking.

where  $H_0$  is the initial height of the fluid without shaking, and  $H$  is the maximum height gained at a given shaking frequency.

### 2.3. Measurement of fluid mixing time

The liquid phase mixing time was measured using a pH tracer method. Reverse osmosis water was adjusted to pH 7.0 and at the start of shaking, 0.5% v/v of 98% concentrated  $H_2SO_4$  (or 2 M NaOH) was added. Fluctuations in the reading of the micro pH probe (VWR International, Leicestershire, UK) inserted in the SUPBr were then monitored until a constant pH value was achieved. The total time taken to achieve a constant pH ( $11$  or  $3 \pm 0.2$ ) was then defined as the mixing time. Each experimental run was carried out in triplicate.

### 2.4. Algal cultivation and maintenance

*Chlorella sorokiniana* was kindly provided by Dr. Saul Purton, Department of Structural and Molecular Biology, University College London and was cultured on tris-base phosphate medium (TBP), modified from Tris–Acetate Phosphate medium “Togasaki and Kropat, 2007”. It had the following stock compositions: 10 mL of  $5 \times$  Beijerincks; 7.5 mM  $NH_4Cl$ , 0.34 mM  $CaCl_2 \cdot 2H_2O$ , 0.4 mM  $MgSO_4 \cdot 2H_2O$ , 8.33 mL of phosphate solution; 0.68 mM  $K_2HPO_4$ , 0.45 mM  $KH_2PO_4$  anhydrous, 100 mL of 2 mM Tris-base, 1 mL of trace elements; 50.0 g EDTA-Na<sub>2</sub>, 11.14 g  $H_3BO_3$ , 22 g  $ZnSO_4 \cdot 7H_2O$ , 5.1 g  $MnCl_2 \cdot 4H_2O$ , 5.0 g  $FeSO_4 \cdot 7H_2O$ , 1.6 g  $CoCl_2 \cdot 6H_2O$ , 1.6 g  $CuSO_4 \cdot 5H_2O$ , 1.1 g  $(NH_4)_6Mo_7O_{24} \cdot 4H_2O$  all dissolved in 1000 mL milliQ water. The seed culture was prepared in two stages. First a *C. sorokiniana* stock (maintained on Nutrient agar slant at 4 °C) was used to inoculate 50 mL TBP medium using 250 mL Erlenmeyer flasks in a Kuhner incubator shaker (Kuhner AG, Switzerland) operated at 180 rpm, 32 °C, and  $55 \mu mol m^{-2} s^{-1}$  for 8 days. For the second stage, 10% v/v of this culture was used to inoculate a new flask following the initial conditions. This was allowed to grow for 4 days and thereafter used for the SUPBr inoculation.

### 2.5. Algae cultivation using the SUPBr

The 2 L SUPBr was aseptically filled with an appropriate working volume of medium and inoculated with  $\sim 5\%$  v/v inoculum. The SUPBr was used with a light intensity of  $180 \pm 20 \mu mol m^{-2} s^{-1}$  and aerated using air enriched with 2% v/v  $CO_2$  at a flow rate of  $0.2 L min^{-1}$ . All experiments were carried out in batch mode with two replicates. Samples (4 mL) were withdrawn at 8 h intervals and stored at  $-20^\circ C$  for analysis.

### 2.6. Analytical methods

#### 2.6.1. Biomass quantification and growth rate calculation

The biomass concentration was determined by optical density measurement at 750 nm using a spectrophotometer (Ultrospec 1100, Amersham Biosciences, UK) and the ammonium concentration measured using a Bioprofile 400 (Nova Biomedical, Cheshire, UK). Biomass dry cell weight was determined using 15 mm diameter Whatman fibre glass filter paper (GE healthcare, UK). A calibration curve was generated and used for the conversion of the optical density readings to mass concentration. Specific growth rate ( $\mu$ ) at exponential phase was determined according to Eq. (2) (Liu et al., 2011):

$$\mu = \frac{\ln X_2 - \ln X_1}{t_2 - t_1} \quad (2)$$

where,  $X_2$  and  $X_1$  are the dry cell weight concentration in ( $g L^{-1}$ ) at time  $t_2$  and  $t_1$  respectively.

#### 2.6.2. Green pigment quantification

A known volume of sample was centrifuged at 10,000 rpm for 10 min (Haematocrit 200, Hettich Zentrifugen, Germany) and the pellet re-suspended in a solution of 90% v/v acetone (Fisher Scientific, Loughborough, UK) and dimethyl sulfoxide (Sigma, UK) in the ratio 3:2 and thereafter allowed to stand for 2 h. The sample was subsequently centrifuged under the same conditions and the  $OD_{750nm}$  of the supernatant measured using a 1 cm path-length quartz cuvette. Concentrations of different pigments were further calculated according to Eqs. 3–5 (Jeffrey and Humphrey, 1975; Pottier et al., 2005):

$$C_{chl-a} = [11.6(OD_{665} - OD_{750}) - 1.31(OD_{645} - OD_{750}) - 0.14(OD_{630} - OD_{750})]V_2I^{-1}(V_1)^{-1} \quad (3)$$

$$C_{chl-b} = 20.7(OD_{645} - OD_{750} - 4.34(OD_{665} - OD_{750}) - 4.42(OD_{630} - OD_{750}))V_2I^{-1}(V_1)^{-1} \quad (4)$$

$$C_{ppc} = [4.42(OD_{480} - OD_{750})]V_2I^{-1}(V_1)^{-1} \quad (5)$$

where,  $V_1$  is the sample volume (1 mL) and  $V_2$  is the volume of the extraction solvent (1 mL). All samples were analysed in triplicate.

#### 2.6.3. Fatty acid methyl ester analysis

Fatty acid methyl esters (FAME) were prepared by direct trans-methylation of lipid extracts in dichloromethane with trimethyl sulfonium hydroxide (TMSH). The FAME were analysed using an XL capillary gas chromatography system (Perkin Elmer Inc., USA) equipped with a flame ionisation detector (FID) and an omegawax 250 capillary column ( $30 m^3$ , 0.25 mm) (Sigma–Aldrich, UK). Nitrogen was used as carrier gas. Initial column temperature was set at 50 °C (2 min), which was subsequently raised to 230 °C at  $4^\circ C min^{-1}$ . The injector was kept as 250 °C with an injection volume of 2  $\mu L$  under split less mode. The FID temperature was set at 260 °C. Individual FAMEs were identified and quantified by comparing their retention times and peak areas with against calibration curves for each FAME.

#### 2.6.4. Calculation of photosynthetic efficiency and biomass yield on irradiance

Calculation of photosynthetic efficiency (PE) was performed using Eq. (6) according to Soletto et al. (2008):

$$PE = \frac{r_G H_G}{IPAR} \times 100 \quad (6)$$

where  $r_G$  is the maximum daily biomass growth ( $g d^{-1}$ ) and  $H_G = 22.9 kJ g_{DCW}^{-1}$  the enthalpy of dry biomass (Morita et al., 2002). IPAR was obtained by multiplying the photosynthetic active radiation (PAR) with the illuminated surface area ( $m^2$ ). A conversion factor of  $18.78 kJ sd^{-1}$  for cool white fluorescent lamps was assumed for the LEDs used in the shaking platform (Soletto et al., 2008). Determination of biomass yield on light energy expressed as dry weight produced per amount of quanta (photons) absorbed in the PAR range ( $Y_{x,E}$ ) was calculated according to Janssen et al. (2003), with the efficiency of light utilisation for photo-autotrophic growth expressed according to Eq. (7):

$$Y_{x,E} = \frac{C_x \mu V}{PFD_{in} A} \quad (7)$$

where,  $C_x$  is the biomass density ( $g L^{-1}$ ),  $\mu$  is the specific growth rate ( $h^{-1}$ ),  $V$  is the liquid volume in the SUPBr ( $m^3$ ),  $PFD_{in}$  is the photo flux density incident on the wall of the SUPBr ( $\mu mol m^{-2} s^{-1}$ ) and  $A$  is the light incident total surface area.

### 3. Results and discussion

#### 3.1. Visualisation of fluid motion in the shaken SUPBr

The fluid hydrodynamics of a rectangular single-use bioreactor, mounted on an orbitally shaken platform, have not previously been investigated. Consequently, initial studies used a high speed video camera to record fluid motion following addition of a dye tracer once a pseudo steady-state flow had been established. ImageJ software was then used to process still images captured at different angles of rotation and to map-out the dispersion of the dye as illustrated in Fig. 2. At low shaking frequencies ( $N < 90$  rpm), the fluid was observed to move in an orbital motion synchronous with the orbital shaking of the platform (Fig. 2(A)). The tracer dye indicated that the fluid flowed sequentially into each corner of the bag during a single orbital rotation gradually becoming more dispersed. This suggests an 'in-phase' fluid motion analogous to that seen in shaken conical flask and microwell bioreactors (Büchs et al., 2001; Micheletti et al., 2006).

At high shaking frequencies ( $N \geq 180$  rpm) the ImageJ analysis indicated a centrally localised region of turbulence (Fig. 2(B)). Here the coloured fluid dispersed in multiple directions simultaneously irrespective of the angle of orbital rotation until it was evenly distributed throughout the entire volume of the fluid. This is similar to the 'out-of-phase' phenomena seen in other shaken bioreactor formats. At intermediate shaking frequencies ( $N > 90$  rpm to  $N < 180$  rpm) there was evidence of a transitional flow regime between these two extremes (data not shown) where the fluid flowed rapidly between opposite corners of the SUPBr. During these experiments, it was noticed that the height attained by the liquid inside the SUPBr correlated with the shaking frequency and the observed fluid flow regime. This was subsequently used as a quantitative metric to explore the observed flow transitions in more detail.

#### 3.2. Determination of in-phase and out-of-phase operating regimes

The fluid dynamics of orbitally shaken bioreactors of various geometries have previously been characterised by the movement

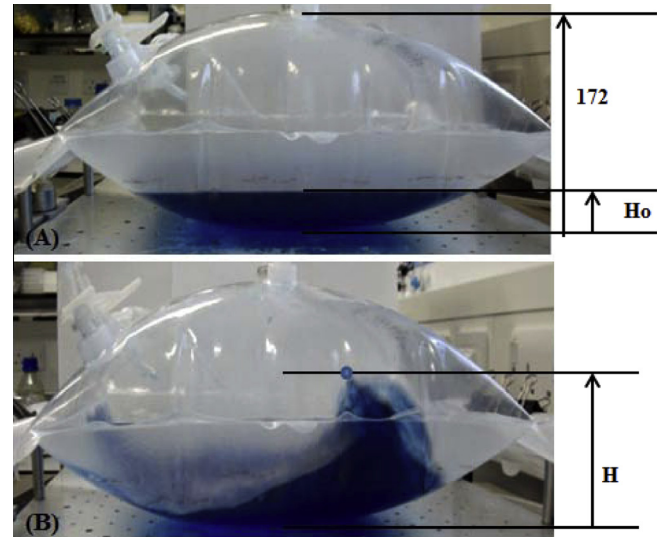


**Fig. 3.** Example images showing (A) the single-use photobioreactor before orbital shaking commenced and (B) the fluid motion and liquid height attained at the experimental conditions:  $N = 220$ ,  $V_f = 0.5$  and  $d_o = 25$  mm.  $H_0$  and  $H$  represent the height attained by the liquid before and after mixing commenced respectively.

of the fluid relative to the shaken platform. In-phase conditions generally result in short mixing times and most often represents favourable operating conditions for cell cultivation. In contrast, out-of-phase conditions are characterised by reduced specific power consumption, poor mixing and gas–liquid mass transfer (Büchs et al., 2000, 2001). In order to better understand these phenomena in the novel SUPBr, the maximum fluid height achieved during shaking was determined from the captured video images as shown in Fig. 3(A and B). The earlier visual observations indicated that the height achieved was indeed a function of shaking frequency, shaking diameter and fluid fill volume.

The measured heights were normalised and plotted against shaking frequency as shown in Fig. 4(A and B) at different orbital shaking diameters. For both diameters and the different fill volumes investigated, the data suggests an almost linear increase in

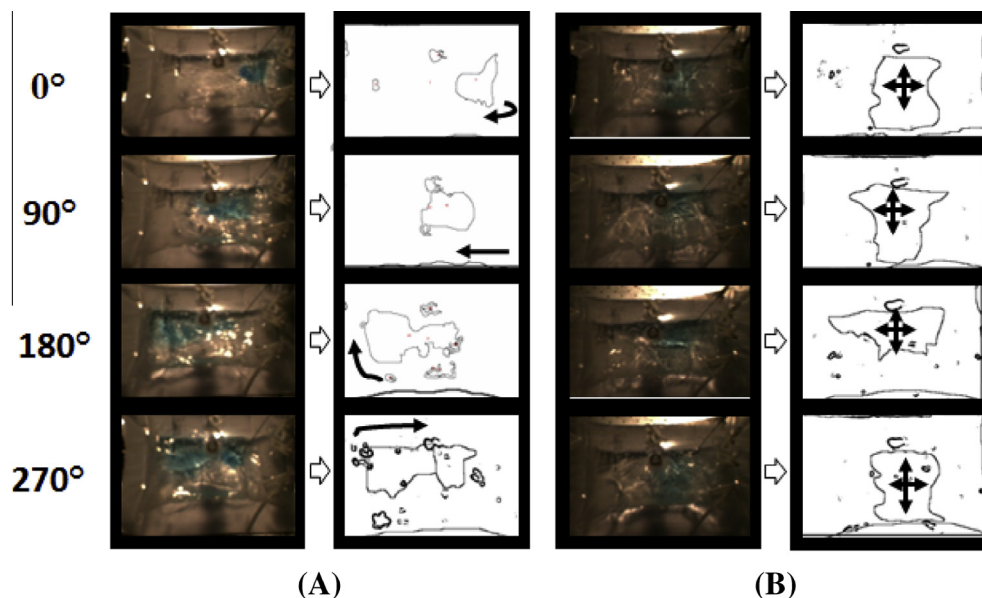


**Fig. 2.** Visualisation of fluid hydrodynamics and schematic representation of dye dispersion in an orbitally shaken Biostat Cultibag™ showing (A) in-phase fluid motion at  $N = 50$  rpm and (B) out-of-phase fluid motion at  $N = 180$  rpm. Arrows indicate generalised direction of liquid flow as observed in the continuous video footage. Experimental conditions:  $V_f = 0.25$ ,  $d_o = 25$  mm.

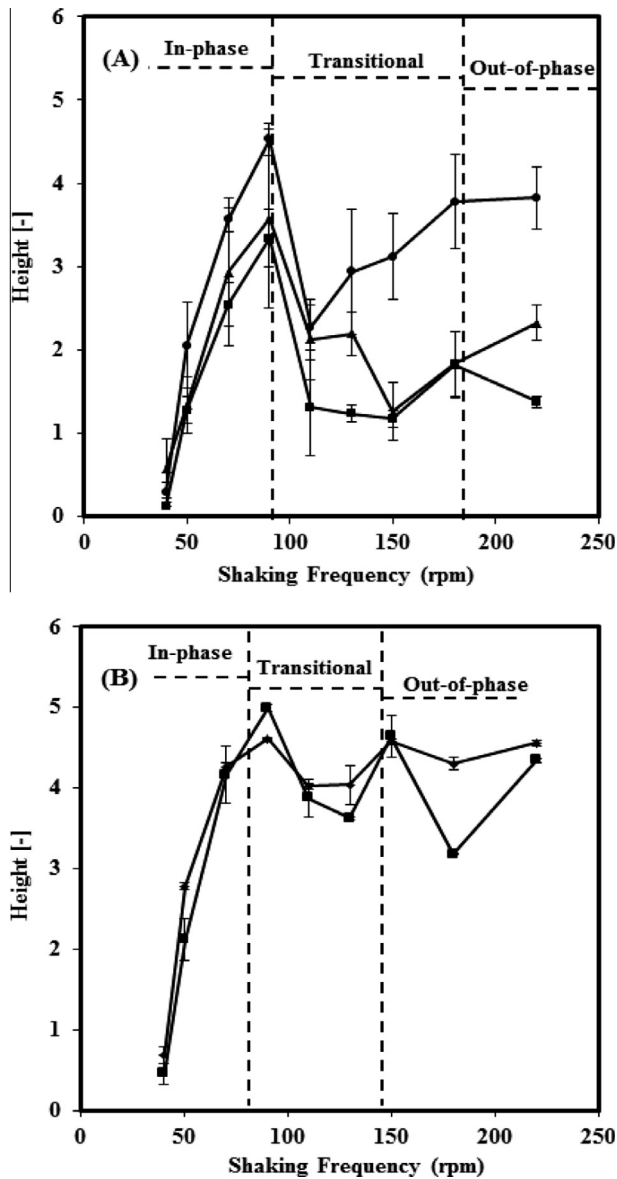


**Fig. 4.** Effect of shaking frequency on fluid hydrodynamics in the single-use photobioreactor (A) at  $d_o = 25$  mm and (B) at  $d_o = 50$  mm. Fill volume fractions ( $V_f$ ) used are: (●) 0.5 (■) 0.25 (▲) 0.1. Error bars represent one standard deviation about the mean ( $n = 3$ ).

the dimensionless height between shaking frequencies of 40–90 rpm. Immediately after 90 rpm the height attained decreases and then attains an approximately constant level for the majority of the conditions studied. Superimposed on Fig. 4(A and B) are the boundaries for the in-phase, transitional and out-of-phase flow patterns described in Section 3.1. These clearly indicate that the range of shaking frequencies over which there is a linear increase in the normalised liquid height corresponds to the in-phase flow regime while out-of-phase conditions resulted in a generally constant liquid height. It therefore becomes interesting to study the impact of these different flow regimes on fluid mixing and algal growth.

### 3.3. Quantification of fluid mixing time

Rapid fluid mixing is normally a pre-requisite for effective bioreactor operation. Efficient mass and heat transfer is generally achieved in bioreactors with shorter mixing times (Micheletti et al., 2006; Tan et al., 2011) and mixing time itself has been found

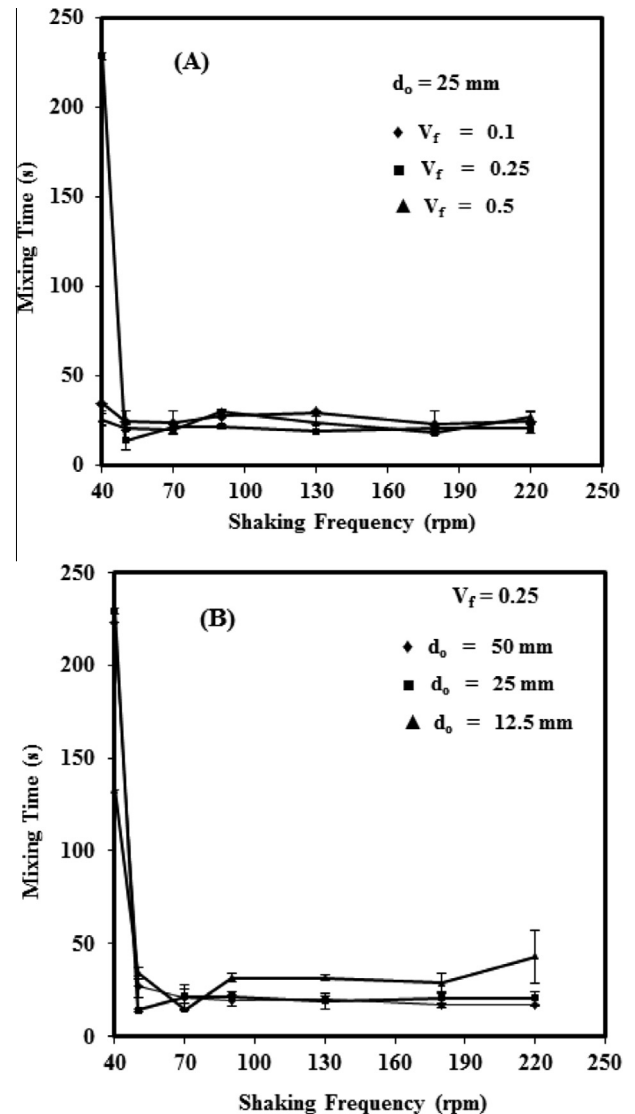


**Fig. 5.** Effect of shaking frequency, fill volume ( $V_f$ ) and orbital shaking diameter ( $d_o$ ) on liquid mixing time,  $t_m$ , in the SUPBr. (A)  $t_m$  at  $d_o = 25$  mm and varying fill volume, and (B)  $t_m$  at  $V_f = 0.25$  with varying  $d_o$ . Error bars represent one standard deviation about the mean ( $n = 3$ ).

to be useful as a scale-up criterion in shaken bioreactor geometries (Betts et al., 2006). Mixing times were quantified using a pH tracer method at varying shaking frequencies (40–220 rpm), fill volume fractions ( $V_f = 0.1$ –0.5) and orbital shaking diameters (12.5, 25 and 50 mm) as shown in Fig. 5(A and B).

At the lowest shaking frequencies investigated (<50 rpm) the mixing time was considerable; up to 230 s, in most cases. At shaking frequencies  $\geq 50$  rpm mixing was rapid and the measured mixing times were approximately constant in the range of 15–30 s for all the fill volumes investigated. Furthermore, comparisons of mixing times determined at different shaking diameters were similar with only slightly higher values being determined at the smaller shaking diameters. Probably the most interesting observation, however, was that at  $\geq 50$  rpm mixing times were small and independent of whether the SUPBr was shaken under in-phase or out-of-phase operating conditions. Similar mixing times were predicted using a more conventional wave mixing platform for 2–20 L bags based on computational fluids dynamics simulations (Oncül et al., 2009). In terms of selecting operating conditions in the SUPBr for algal cultivation, operation at shaking diameters of 25 or 50 mm

and at lower fill volumes, i.e. 0.25, are recommended given the rapid mixing, large gas–liquid area per unit liquid volume for gas mass transfer and the reduced light path-length for light penetration into densely growing cultures.

### 3.4. *C. sorokiniana* growth kinetics in the SUPBr

The growth kinetics of *C. sorokiniana* were subsequently examined over a range of SUPBr operating conditions. *C. sorokiniana* was chosen because of its robustness and easy handling (Liu et al., 2013). Cultures were performed at a constant light intensity of  $\sim 180 \pm 20 \mu\text{mol m}^{-2} \text{s}^{-1}$  using air enriched with 2% v/v  $\text{CO}_2$  as carbon source which was provided via head space surface aeration. The growth medium was modified and optimised in separate small scale experiments (data not shown), by replacing the tris–acetate with 0.2 M tris–base, in order to buffer pH changes during culture between 7.04 and 5.80 (Kumar and Das, 2012). Early stationary phase cultures were used for inoculating the shaken SUPBr (Mattos et al., 2012) and Nitrogen concentration was kept low to

allow early production of lipid at the mid-exponential phase; a technique widely used to ensure high biomass yield and lipid production with a high linoleic acid concentration which is a key requirement for biodiesel production (Chader et al., 2011; Cordero et al., 2011).

Biomass concentration profiles at different shaking frequencies showed a short lag phase during day one, followed by an exponential phase before reaching stationary phase after 3 days. The final biomass yield was  $6.6 \text{ g L}^{-1}$  at 180 rpm (Fig. 6(A)). Shaking frequencies above or below this do not have a significant influence on growth kinetics at constant light intensity and working volume. As shown in Fig. 6(B) the initial ammonium concentration (7 mM) was sufficient to support cell growth over day 1–2 and was depleted by day 2–3 after which lipid accumulation occurred. Fig. 6(B) also shows pH was maintained constant between 7.0 and 5.8 as a consequence of reformulating the media.

Fill volume was expected to have a more significant influence on SUPBr performance due to increase in the liquid depth, i.e. increased light path length, and reduction in surface area to

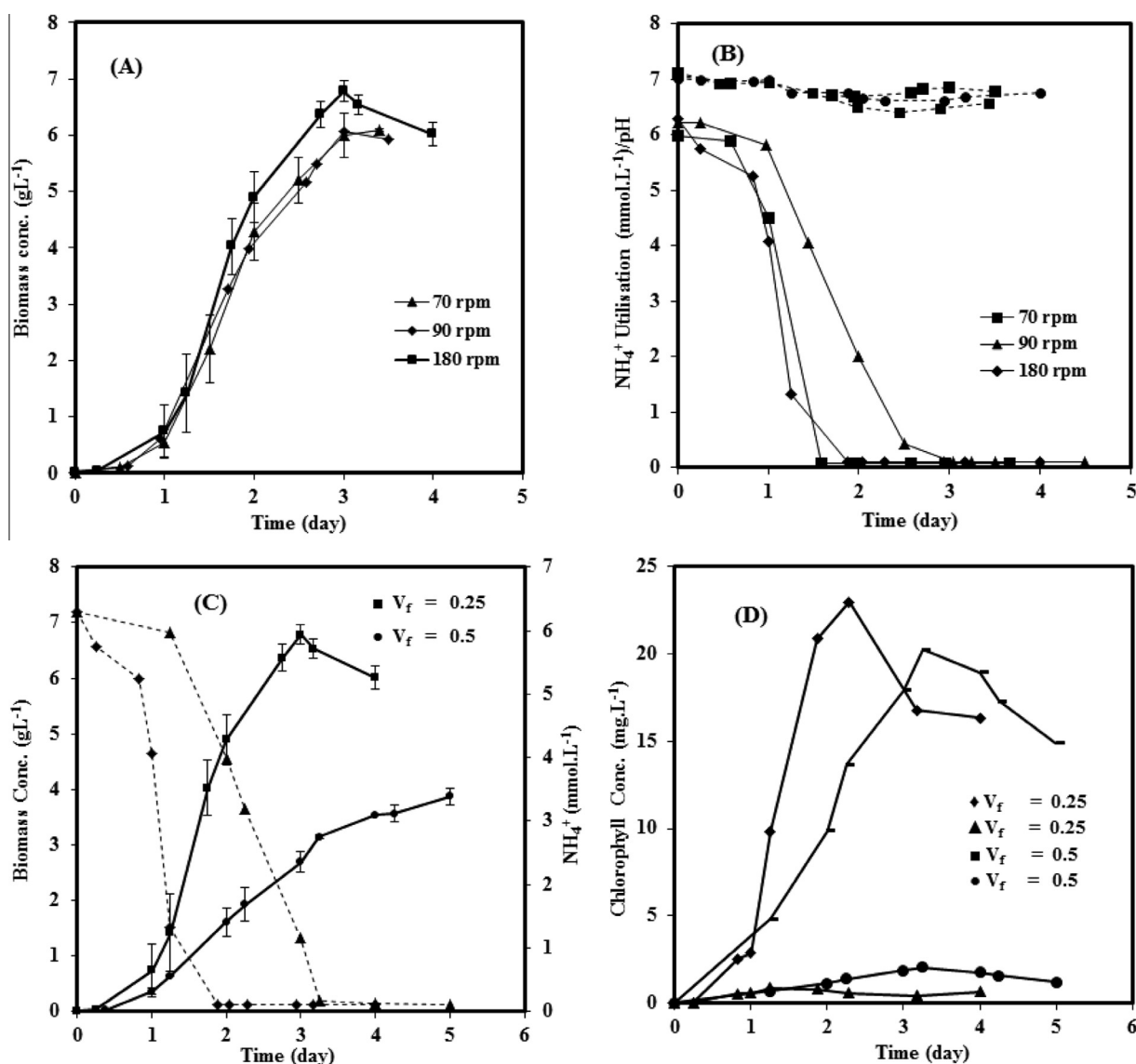


**Fig. 6.** Impact of shaking frequency and fill volume on growth kinetics of *C. sorokiniana*: (A) biomass concentration, (B)  $\text{NH}_4^+$  utilisation and pH at  $V_f = 0.25$  and different shaking frequencies: (▲) 70 rpm (◆) 90 rpm (■) 180 rpm (●) 90 rpm ( $V_f = 0.5$ ). (C) Effect of fill volume on growth kinetics and Nitrogen consumption. Biomass concentration at (●)  $V_f = 0.5$  and (■)  $V_f = 0.25$  and Nitrogen uptake kinetics at (▲)  $V_f = 0.5$  and (◆)  $V_f = 0.25$ ; (D) effect of fill volume on chlorophyll 'a' and carotenoids concentration at (■)  $V_f = 0.5$  and (◆)  $V_f = 0.25$  at  $N = 180$  rpm. Error bars represent one standard deviation about the mean ( $n = 3$ ).

**Table 1**Summary of *C. sorokiniana* growth kinetics at different shaking frequencies and fill volumes in a 2 L orbitally shaken Biostat Cultibag™ (irradiance 180  $\mu\text{mol m}^{-2} \text{s}^{-1}$ ).

Growth parameters	Fill volume					
	$V_f = 0.25$					$V_f = 0.50$
Shaking frequency (rpm)	70	90	130	180	220	180
Specific growth rate ( $\text{h}^{-1}$ )	0.05	0.05	0.09	0.11	0.12	0.02
Biomass conc. ( $\text{g L}^{-1}$ )	6.00	6.07	6.05	6.61	6.23	4.11
Biomass productivity ( $\text{g L}^{-1} \text{day}^{-1}$ )	2.00	2.02	2.02	2.25	2.08	0.82
Photosynthetic efficiency (%)	17.68	16.53	16.53	18.41	17.02	6.73
$Y_{x,E}$ ( $\text{g mol photons}^{-1}$ )	1.55	1.57	2.81	3.76	3.86	NA

 $V_f$ : fractional fill volume of total SUPBr volume.

\* NA: not available.

**Table 2**Impact of SUPBr operating conditions on fatty acid methyl ester (FAME) production by *C. sorokiniana*. Error represents one standard deviation about the mean ( $n = 3$ ). Growth conditions as described in Fig. 6.

Fatty acids (wt% of identified FAME)	Structural formulae	Shaking frequency (rpm) ( $V_f = 0.25$ )			
		70	180	220	180 rpm ( $V_f = 0.5$ )
Capric acid	C10:0	8.51 $\pm$ 2.76	0.16 $\pm$ 0.10	1.62 $\pm$ 0.25	0.82 $\pm$ 0.06
Lauric acid	C12:0	0.11 $\pm$ 0.04	0.17 $\pm$ 0.15	0.09 $\pm$ 0.04	0.12 $\pm$ 0.00
Myristic acid	C14:0	0.56 $\pm$ 0.05	0.56 $\pm$ 0.02	0.64 $\pm$ 0.05	0.83 $\pm$ 0.01
Palmitic acid	C16:0	27.18 $\pm$ 14.5	35.12 $\pm$ 1.42	33.80 $\pm$ 2.07	36.71 $\pm$ 0.71
Palmitoleic acid	C16:1	3.39 $\pm$ 0.30	3.60 $\pm$ 0.15	4.42 $\pm$ 0.28	5.16 $\pm$ 0.11
Heptadecanoic acid	C17:0	0.36 $\pm$ 0.03	0.33 $\pm$ 0.01	0.22 $\pm$ 0.01	0.22 $\pm$ 0.01
cis-10-Heptadecanoic acid	C17:1	3.79 $\pm$ 0.33	4.12 $\pm$ 0.20	4.32 $\pm$ 0.28	3.91 $\pm$ 0.09
Stearic acid	C18:0	2.13 $\pm$ 0.18	2.26 $\pm$ 0.12	2.73 $\pm$ 0.16	2.80 $\pm$ 0.07
Oleic/elaidic acid	C18:1n9c-t	16.01 $\pm$ 1.34	14.77 $\pm$ 0.75	15.65 $\pm$ 0.91	17.58 $\pm$ 0.43
Linoleic acid	C18:2n6c	30.02 $\pm$ 0.00	32.05 $\pm$ 1.62	28.22 $\pm$ 1.69	27.39 $\pm$ 0.61
Linolelaidic acid	C18:2n6t	0.92 $\pm$ 0.27	0.15 $\pm$ 0.01	0.06 $\pm$ 0.00	0.20 $\pm$ 0.01
$\gamma$ -Linoleic acid	C18:3n6	0.11 $\pm$ 0.02	4.57 $\pm$ 0.25	4.52 $\pm$ 0.28	2.94 $\pm$ 0.07
$\alpha$ -Linoleic acid	C18:3n3	4.64 $\pm$ 0.42	1.40 $\pm$ 0.14	2.08 $\pm$ 0.11	0.00 $\pm$ 0.00
Active biofuel components	C16–C18	88.54	98.34	96.02	96.92
Saturated fatty acids	SFA	41.80	39.50	40.49	43.04
Monounsaturated fatty acids	MUFA	23.52	22.48	24.72	26.71
Poly-unsaturated fatty acids	PUFA	35.68	38.15	34.88	30.53
Unsaturated fatty acids (MUFA + PUFA)	UFA	59.20	60.64	59.60	57.24
Ratio of unsaturated to saturated fatty acids	UFA:SFA	1.42	1.54	1.47	1.33

volume ratio at higher fill volumes. Other expected effects at increased cell density include cell shadowing that can lead to reduced cell growth rate (Cuaresma et al., 2009). As shown in Fig. 6(C), doubling the total liquid volume ( $V_f$  increases from 0.25 to 0.5) led to a decrease in algal growth rate and yield resulting in a calculated decrease in biomass productivity of approximately 35–40%. The decreased biomass growth also coincided with a decreased rate of Nitrogen utilisation and decreased chlorophyll productivity (Fig. 6(D)). Over all the conditions investigated, maximum chlorophyll concentration varies between 20 and 25  $\text{mg L}^{-1}$ .

The percentage total lipid formation across the various shaking frequencies range between 18 and 28% ( $\text{g lipid}^{-1} \text{g mass}$ ), comparable to results obtained by Wan et al. (2011), where, *C. sorokiniana* was cultured mixotrophically with zero initial glucose concentration. Nitrogen deprivation has been reported to improve the lipid content (Hsieh and Wu, 2009) which was also confirmed by the result obtained in this work. The total lipids extracted from *C. sorokiniana* have been estimated to consist of approximately 93% of neutral lipids with the rest being polar lipids (Zheng et al., 2013). For growth in a simulated open pond photobioreactor Bellou and Aggelis (2012) reported 7–8.3% ( $\text{g lipid g mass}^{-1}$ ) for *C. sorokiniana* sp. which was comparatively lower than the amount reported here, while the proportion of neutral lipid obtained was about 50% lower than compared to Zheng et al. (2013).

Evaluation of different growth parameters as shown in Table 1 reveals that at constant fill volume and light intensity, no significant differences were observed in growth parameters at different

shaking frequencies up to 180 rpm. This agrees with the mixing time studies discussed previously in Section 3.3. However, operation at a higher frequency of 220 rpm resulted in a slight reduction of biomass concentration and PE. Doubling the fill volume at the optimum shaking frequency (180 rpm) resulted in significant reduction in all the growth parameters assessed. These results further show how important are light path length, surface area to volume ratio and fluid hydrodynamics in SUPBr design. The biomass yield on photon absorption ( $Y_{x,E}$ ) shows an increase with increasing shaking frequency and may be due to increased exposure of the cells to light.

Similar results were reported by Cordero et al. (2011), using Roux flasks laterally illuminated using a mercury halide lamp at varying luminous intensity. Comparison of the specific growth rate and biomass concentration varied between 0.05–0.13  $\text{h}^{-1}$ , and 6.0–9.0  $\text{g L}^{-1}$  respectively. Despite slight differences in some of the operating parameters used, improved culture performance was observed in the SUPBr compared to other similar system previously reported (Chiu et al., 2008; Kumar and Das, 2012; Ugwu et al., 2005). In addition, studies showed that cultivation of *C. sorokiniana* in a flat panel photobioreactor under continuous conditions gave a biomass concentration of 5.7  $\text{g L}^{-1}$  at the lowest dilution rate (Cuaresma et al., 2009). Comparing the SUPBr data with other optimised photo-bioreactors of different geometry suggests the SUPBr offers potential advantages in terms of biomass productivity, reduction in process time and reduced chances of contamination.

### 3.5. Fatty acid methyl ester composition

The lipid compositions of the algae cultured under various conditions were also determined to ensure consistency. The different FAMES analysed were grouped based on the degree of saturation and unsaturation such as; saturated fatty acids (SFA), monounsaturated fatty acids (MUFA) and poly-unsaturated fatty acids (PUFA). For all the different culture conditions tested, palmitic acid methyl ester (PAME) was amongst the most prevalent. Approximately,  $33 \pm 3.6\%$  PAME and  $41.21 \pm 1.3\%$  SFA of the total identified FAME were produced as shown in Table 2. These results are comparable with those obtained by Lu et al. (2012) and Zheng et al. (2013) which are 36.1–42.8% and 45.6% SFA respectively. Work done by Cha et al. (2011), shows about a two fold increase in the SFA achieved under varied concentration of nitrate, with 86.3% of SFA produced at 0.18 mM nitrate concentration compared to the 7.5 mM ammonium salt employed in this study. This could be indicative of the impact of Nitrogen source and concentration on the SFA production. Nonetheless, this study shows that the total amount of SFA produced is independent of the fill volume and shaking frequencies.

Unsaturated fatty acids correspond to ~60.6% of total FAME. These comprise of the mono-unsaturated fatty acids (MUFA) and PUFA with individual percentage compositions in the range of 22.5–26.7% and 30.5–38.2% respectively across all conditions. FAME with C16 and C18 chain lengths have found more direct application to the biofuel industry than others. Estimation of the total percentage of C16 and C18 carbon chain length shows 98% of total FAME with PAMES (C16:0) and linoleic acid methyl esters (C18:2n6c) forming the major constituents for biodiesel production. From the results shown (Table 2), the biodiesel component of the FAME increased with increasing frequency up to 180 rpm. This suggests that under more agitated conditions, higher biodiesel required components are produced. On the contrary, the effect of fill volume was insignificant on the percentage composition of the C16–C18 components. Other FAME produced of pharmaceutical importance includes capric acid, lauric acid, myristoleic acid, palmitoleic acids and stearic acid methyl esters (Prathima Devi et al., 2012). Eicosapentaenoic acid methyl esters (EPA) were not detected at any of the tested conditions; this may be due to the absence of acetate in the medium which might be a key metabolic precursor for the production of FAME of higher carbon chain length of C20 and above.

## 4. Conclusions

This work described a novel, orbitally shaken, SUPBr suitable for early stage development of microalgal cultivation processes. In terms of the engineering environment within the SUPBr, orbital shaking provides rapid mixing and a relatively constant light intensity while the surface area to volume ratio enhances effective gas mass transfer. Various flow regimes were identified as a function of shaking frequency however the main factor influencing culture productivity was the liquid fill volume due to its influence on light path-length. Further studies should address scale translation and the ability to predict algal growth kinetics as seen in industrial scale, bag-based photobioreactors.

## Acknowledgements

EO would like to acknowledge the Nigerian Petroleum Technology Development Fund (PTDF) for award of a doctoral studentship. The authors would also like to thank Infors HT for their advice and modifications to the shaking platform and the EPSRC Equipment Loan Pool for use of the high speed video cameras.

## References

- Bellou, S., Aggelis, G., 2012. Biochemical activities in *Chlorella* sp. and *Nannochloropsis salina* during lipid and sugar synthesis in a lab-scale open pond simulating reactor. *J. Biotechnol.* 164, 318–329. <http://dx.doi.org/10.1016/j.biotech.2013.01.010>.
- Betts, J.L., Doig, S.D., Baganz, F., 2006. Characterization and application of a miniature 10 mL stirred-tank bioreactor, showing scale-down equivalence with a conventional 7 L reactor. *Biotechnol. Prog.* 22, 681–688. <http://dx.doi.org/10.1021/bp050369y>.
- Brecht, R., 2009. Disposable bioreactors: maturation into pharmaceutical glycoprotein manufacturing. *Adv. Biochem. Eng. Biotechnol.* 115, 1–31. <http://dx.doi.org/10.1007/10>.
- Büchs, J., Lotter, S., Milbradt, C., 2001. Out-of-phase operating conditions, a hitherto unknown phenomenon in shaking bioreactors. *Biochem. Eng. J.* 7, 135–141.
- Büchs, J., Maier, U., Milbradt, C., Zoels, B., 2000. Power consumption in shaking flasks on rotary shaking machines: I. Power consumption measurement in unbaffled flasks at low liquid viscosity. *Biotechnol. Bioeng.* 68, 589–593.
- Cha, T.S., Chen, J.W., Goh, E.G., Aziz, A., Loh, S.H., 2011. Differential regulation of fatty acid biosynthesis in two *Chlorella* species in response to nitrate treatments and the potential of binary blending microalgae oils for biodiesel application. *Bioresour. Technol.* 102, 10633–10640. <http://dx.doi.org/10.1016/j.biortech.2011.09.042>.
- Chader, S., Mahmah, B., Chetehouna, K., Mignolet, E., 2011. Biodiesel production using *Chlorella sorokiniana* a green microalga. *Rev. Energies Renouvelables* 14, 21–26.
- Chen, C.-Y., Yeh, K.-L., Aisyah, R., Lee, D.-J., Chang, J.-S., 2011. Cultivation, photobioreactor design and harvesting of microalgae for biodiesel production: a critical review. *Bioresour. Technol.* 102, 71–81. <http://dx.doi.org/10.1016/j.biortech.2010.06.159>.
- Chiu, S.-Y., Kao, C.-Y., Chen, C.-H., Kuan, T.-C., Ong, S.-C., Lin, C.-S., 2008. Reduction of CO<sub>2</sub> by a high-density culture of *Chlorella* sp. in a semicontinuous photobioreactor. *Bioresour. Technol.* 99, 3389–3396.
- Cordero, B.F., Obratsova, I., Couso, I., Leon, R., Vargas, M.A., Rodriguez, H., 2011. Enhancement of lutein production in *Chlorella sorokiniana* (Chlorophyta) by improvement of culture conditions and random mutagenesis. *Mar. Drugs* 9, 1607–1624. <http://dx.doi.org/10.3390/md9091607>.
- Cuaresma, M., Janssen, M., Vilchez, C., Wijffels, R.H., 2009. Productivity of *Chlorella sorokiniana* in a short light-path (SLP) panel photobioreactor under high irradiance. *Biotechnol. Bioeng.* 104, 352–359. <http://dx.doi.org/10.1002/bit.22394>.
- Hillig, F., Porscha, N., Junne, S., Neubauer, P., 2014. Growth and docosahexaenoic acid production performance of the heterotrophic marine microalgae *Cryptocodinium cohnii* in the wave-mixed single-use reactor CELL-tainer. *Eng. Life Sci.* 14, 254–263. <http://dx.doi.org/10.1002/elsc.201400010>.
- Hsieh, C.-H., Wu, W.-T., 2009. Cultivation of microalgae for oil production with a cultivation strategy of urea limitation. *Bioresour. Technol.* 100, 3921–3926. <http://dx.doi.org/10.1016/j.biortech.2009.03.019>.
- Janssen, M., Tramper, J., Mur, L.R., Wijffels, R.H., 2003. Enclosed outdoor photobioreactors: light regime, photosynthetic efficiency, scale-up, and future prospects. *Biotechnol. Bioeng.* 81, 193–210. <http://dx.doi.org/10.1002/bit.10468>.
- Jeffrey, S.W., Humphrey, G.F., 1975. New spectrophotometric equations for determining chlorophyll a, b, c1 and c2 in higher plants, algae and natural phytoplankton. *Biochem. Physiol. Pflanz* 167, 191–194.
- Kalmbach, A., Bordás, R., Oncül, A.A., Thévenin, D., Genzel, Y., Reichl, U., 2011. Experimental characterization of flow conditions in 2- and 20-L bioreactors with wave-induced motion. *Biotechnol. Prog.* 27, 402–409. <http://dx.doi.org/10.1002/btpr.516>.
- Kumar, K., Das, D., 2012. Growth characteristics of *Chlorella sorokiniana* in airlift and bubble column photobioreactors. *Bioresour. Technol.* 116, 307–313. <http://dx.doi.org/10.1016/j.biortech.2012.03.074>.
- Lehmann, N., Rischer, H., Eibl, D., Eibl, R., 2013. Wave-mixed and orbitally shaken single-use photobioreactors for diatom algae propagation. *Chem. Ing. Tech.* 85, 197–201. <http://dx.doi.org/10.1002/cite.201200137>.
- Liu, J., Huang, J., Sun, Z., Zhong, Y., Jiang, Y., Chen, F., 2011. Differential lipid and fatty acid profiles of photoautotrophic and heterotrophic *Chlorella zofingiensis*: assessment of algal oils for biodiesel production. *Bioresour. Technol.* 102, 106–110. <http://dx.doi.org/10.1016/j.biortech.2010.06.017>.
- Liu, T., Wang, J., Hu, Q., Cheng, P., Ji, B., Liu, J., Chen, Y., Zhang, W., Chen, X., Chen, L., Gao, L., Ji, C., Wang, H., 2013. Attached cultivation technology of microalgae for efficient biomass feedstock production. *Bioresour. Technol.* 127, 216–222. <http://dx.doi.org/10.1016/j.biortech.2012.09.100>.
- Lu, S., Wang, J., Niu, Y., Yang, J., Zhou, J., Yuan, Y., 2012. Metabolic profiling reveals growth related FAME productivity and quality of *Chlorella sorokiniana* with different inoculum sizes. *Biotechnol. Bioeng.* 109, 1651–1662. <http://dx.doi.org/10.1002/bit.24447>.
- Mattos, E.R., Singh, M., Cabrera, M.L., Das, K.C., 2012. Effects of inoculum physiological stage on the growth characteristics of *Chlorella sorokiniana* cultivated under different CO<sub>2</sub> concentrations. *Appl. Biochem. Biotechnol.* 168, 519–530. <http://dx.doi.org/10.1007/s12010-012-9793-6>.
- Micheletti, M., Barrett, T., Doig, S., Baganz, F., Levy, M., Woodley, J., Lye, G., 2006. Fluid mixing in shaken bioreactors: implications for scale-up predictions from microlitre-scale microbial and mammalian cell cultures. *Chem. Eng. Sci.* 61, 2939–2949. <http://dx.doi.org/10.1016/j.ces.2005.11.028>.

- Morita, M., Watanabe, Y., Saiki, H., 2002. Photosynthetic productivity of conical helical tubular photobioreactor incorporating *Chlorella sorokiniana* under field conditions. *Biotechnol. Bioeng.* 77, 155–162. <http://dx.doi.org/10.1002/bit.10119>.
- Oncül, A.A., Kalmbach, A., Genzel, Y., Reichl, U., Thévenin, D., 2009. Characterization of flow conditions in 2 L and 20 L wave bioreactors using computational fluid dynamics. *Biotechnol. Prog.* 26, 101–110. <http://dx.doi.org/10.1002/btpr.312>.
- Pottier, L., Pruvost, J., Deremetz, J., Cornet, J.-F., Legrand, J., Dussap, C.G., 2005. A fully predictive model for one-dimensional light attenuation by *Chlamydomonas reinhardtii* in a torus photobioreactor. *Biotechnol. Bioeng.* 91, 569–582.
- Prathima Devi, M., Venkata Subhash, G., Venkata Mohan, S., 2012. Heterotrophic cultivation of mixed microalgae for lipid accumulation and wastewater treatment during sequential growth and starvation phases: effect of nutrient supplementation. *Renew. Energy* 43, 276–283. <http://dx.doi.org/10.1016/j.renene.2011.11.021>.
- Singh, V., 1999. Disposable bioreactor for cell culture using wave-induced agitation. *Cytotechnology* 30, 149–158. <http://dx.doi.org/10.1023/A:1008025016272>.
- Soletto, D., Binaghi, L., Ferrari, L., Lodi, A., Carvalho, J.C.M., Zilli, M., Converti, A., 2008. Effects of carbon dioxide feeding rate and light intensity on the fed-batch pulse-feeding cultivation of *Spirulina platensis* in helical photobioreactor. *Biochem. Eng. J.* 39, 369–375. <http://dx.doi.org/10.1016/j.bej.2007.10.007>.
- Tan, R., Eberhard, W., Jochen, B., 2011. Measurement and characterization of mixing time in shake flasks. *Chem. Eng. Sci.* 66, 440–447. <http://dx.doi.org/10.1016/j.ces.2010.11.001>.
- Tissot, S., Farhat, M., Hacker, D.L., Anderlei, T., Kühner, M., Comminellis, C., Wurm, F., 2010. Determination of a scale-up factor from mixing time studies in orbitally shaken bioreactors. *Biochem. Eng. J.* 52, 181–186. <http://dx.doi.org/10.1016/j.bej.2010.08.005>.
- Ugwu, C.U., Ogbonna, J.C., Tanaka, H., 2005. Light/dark cyclic movement of algal culture (*Synechocystis aquatilis*) in outdoor inclined tubular photobioreactor equipped with static mixers for efficient production of biomass. *Biotechnol. Lett.* 27, 75–78. <http://dx.doi.org/10.1007/s10529-004-6931-4>.
- Wan, M., Liu, P., Xia, J., Rosenberg, J.N., Oyler, G.A., Betenbaugh, M.J., Nie, Z., Qiu, G., 2011. The effect of mixotrophy on microalgal growth, lipid content, and expression levels of three pathway genes in *Chlorella sorokiniana*. *Appl. Microbiol. Biotechnol.* 91, 835–844. <http://dx.doi.org/10.1007/s00253-011-3399-8>.
- Zhang, Q., Yong, Y., Mao, Z.-S., Yang, C., Zhao, C., 2009. Experimental determination and numerical simulation of mixing time in a gas-liquid stirred tank. *Chem. Eng. Sci.* 64, 2926–2933. <http://dx.doi.org/10.1016/j.ces.2009.03.030>.
- Zheng, Y., Li, T., Yu, X., Bates, P.D., Dong, T., Chen, S., 2013. High-density fed-batch culture of a thermotolerant microalga *Chlorella sorokiniana* for biofuel production. *Appl. Energy* 108, 281–287. <http://dx.doi.org/10.1016/j.apenergy.2013.02.059>.